

Direct experimental evidence of insensitivity of local Schottky barriers to lateral chemical inhomogeneity in case studies of metal/GaN(0001) interfaces

A. Barinov, L. Gregoratti, and M. Kiskinova
Sincrotrone Trieste, Area Science Park, 34012-Trieste, Italy
 (Received 10 September 2001; published 30 October 2001)

The response of local Schottky barriers (SB) to local specifics of the interface is readdressed by photoelectron microscopy investigations of metal/GaN interfaces, which reveal that compositional and morphological inhomogeneities have no effect on local SB heights. This unexpected behavior is ascribed to lateral charge redistribution between different interface regions leading to homogenization of the SB fluctuations at the semiconductor surface in contact with the metallic layer.

DOI: 10.1103/PhysRevB.64.201312

PACS number(s): 73.30.+y, 68.37.Xy, 68.55.Nq, 79.60.Jv

Despite the intensive investigations, over a century, the basic mechanism which determines the Schottky barriers (SB) at metal-semiconductor (M/S) interfaces is still an open issue. Several competing models have tried to explain the experimentally measured SB values. Most of the models treat the SB formation in terms of a Fermi level (FL) pinning, but still there is no consensus about the key factors affecting the FL position within the band gap, namely whether it is determined by *intrinsic* interface electronic states or by *extrinsic* defect-related states, and how the electron transport at the interface is affected by exchange reactions, structural rearrangements and lateral inhomogeneity.¹⁻⁶ Studies of the effect of interface morphology on the SB predict that only the top semiconductor layers have a sizable effect on the FL pinning.^{5,6} On the other hand, recent theoretical work excludes the possibility of FL pinning at M/GaN interfaces. The authors conclude that the interface dipole, determined by the structural arrangement of the first metal layer, cannot be properly screened and controls the SB height of M/GaN interfaces.⁷

One of the most serious complications in the elucidation of the mechanisms involved in the SB formation is that, as stated in most studies, a uniform interface morphology is an idealized case. Real M/S interfaces are not perfect and contain structural and/or chemical heterogeneities that can introduce spatial fluctuations in the SB height. Models explaining the nonideal behavior of the Schottky diodes and the dependence of the SB height on the doping level and measurement methods¹⁻⁴ in terms of different local FL pinning, determined by the local interface specifics, are not applicable for interfaces with unpinning FL. An additional difficulty in treating the effect of microscopic morphology on the electron transport at M/S interfaces is that interactions between adjacent regions with different electronic properties should be considered as well.

Essential for elucidation inhomogeneity effects is direct experimental access to the lateral variations of the interface composition and band bending (BB). One of the promising methods used recently for measuring the SB inhomogeneity is ballistic electron emission microscopy (BEEM).⁸⁻¹¹ BEEM has an atomic resolution but lacks surface and chemical sensitivities. This is a serious weakness because the lateral SB fluctuations are predicted as a natural result of inhomogeneity of the structure and chemical composition of the

interface. Apparently, quantitative understanding of the factors contributing to the SB inhomogeneity requires a technique capable of probing both the local composition of the M/S interface and the corresponding BB at the surface. This requirement is met by adding submicrometer lateral resolution to photoelectron spectroscopy, a chemically sensitive method where the probing depth can easily be set to less than 50 Å.^{1,12,13} The determination of the SB height is based on the simple mechanism of band bending, which leads to an energy shift of the photoelectron (PE) spectrum and does not depend on the transport mechanisms across the barrier.¹² Although the spatial resolution of photoelectron microscopes, 50–100 nm, is less than that of BEEM, they have already demonstrated their potential in studies of heterogeneous interfaces.^{13,14}

Our studies of M/GaN systems have been motivated by reports in which lateral variations of the electronic properties of M/GaN interfaces, induced by the defect structure of the GaN films, are held responsible for the unstable performance of technologically important GaN-based devices.^{15,16} The theoretical predictions that structural differences between the M/GaN interfaces play a more important role than metal electronegativity also render the M/GaN interfaces interesting model systems for probing the SB inhomogeneity.⁷ In the framework of these predictions our results that the chemical lateral heterogeneity, induced by annealing of Au/GaN and Ni/GaN interfaces has a negligible effect on the local SB, seemed rather surprising.^{17,18} With the present study of a highly reactive Ti/GaN interface we confirm the insensitivity of the SB to the local specifics of M/GaN(0001) interfaces, a finding that stimulates reconsideration of the factors contributing to the transport properties across M/S junctions.

All experiments were carried out with a spatial resolution of 0.12 μm using the zone-plate based scanning photoelectron microscope (SPEM) at the ELETTRA synchrotron light source.¹⁹ The SPEM has two operation modes, imaging by collecting photoelectrons with a specified kinetic energy while scanning the sample, and spectroscopy from a microspot. The contrast of the images reflects the lateral variation in the photoelectron yield within the chosen energy window. The electron levels energy shifts are the fingerprints used for elucidating the elemental chemical state and BB. The SPEM spectral resolution of 0.3 eV allows determination of the BB-related energy shifts of the Ga 3*d* core lines

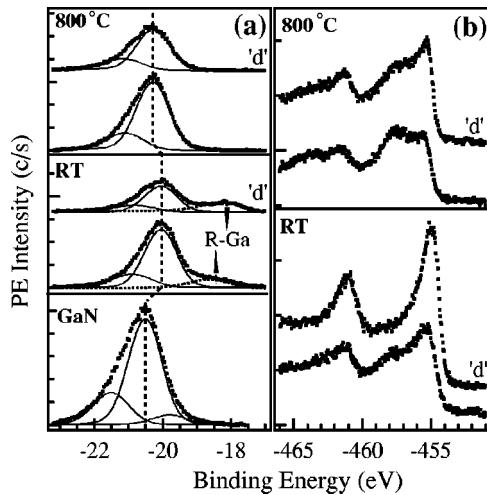


FIG. 1. Ga 3d (a) and Ti 2p (b) spectra taken from different regions of the laterally heterogeneous Ti/GaN interface at RT and after annealing to 800 °C. The spectra from the Ti-enriched regions are indicated by “d”. The dashed line indicates the BB-induced shifts of the GaN-related peak. The Ga 3d spectrum of an atomically clean GaN surface is shown in the bottom panel of (a).

of GaN with accuracy better than 0.05 eV. The binding energies (BE) of the atomic levels are referred to the equilibrium FL, measured on the Ta clips holding the sample. The SPEM station is equipped with facilities for *in situ* specimen preparation and characterization by low energy electron diffraction (LEED) and Auger electron spectroscopy (AES).

The samples, $\sim 0.5\text{--}1.0\ \mu\text{m}$ GaN epitaxial layers grown on highly-doped Si or SiC substrates, had a high natural *n*-doping level ($\geq 5 \times 10^{16}\ \text{cm}^{-3}$) and carrier mobility ($\geq 500\ \text{V}^{-1}\ \text{cm}^2\ \text{s}^{-1}$) and did not charge-up. Atomically clean GaN surface, confirmed by the AES and PE spectra, was obtained by cycles of N_2 ion sputtering (0.6 kV) and annealing to 850 °C. The Ga 3d, N 1s and valence-band spectra of the clean GaN surface were very similar to those previously measured and theoretically predicted.^{20–24} The Ga 3d spectrum, shown in Fig. 1(a), requires two GaN fitting components, which account for the band dispersion of the Ga 3d semicore levels.^{23,24} The energy shifts of these components, which preserve their line shape, energy separation and intensity ratio after metal deposition and interfacial reactions, are used as a measure of the local BB. There is also a small surface component, shifted by $\sim 0.6\ \text{eV}$, which disappeared after metal deposition.

Metal films were deposited through masks, leaving a metal-free GaN surface as a reference. Here the interface was formed by deposition of 5 Å Ti on a clean GaN(0001) at room temperature (RT). For the used photon energy of 585 eV and detection geometry the escape depth of Ti 2p, N 1s, and Ga 3d photoelectrons is $\sim 2.5, 2.8,$ and $5.2\ \text{Å}$, respectively, which means that our effective probing depth is less than 20 Å.

By mapping different areas of the reactive Ti/GaN interface after Ti deposition we found Ti-enriched regions with preferential orientation along the main crystallographic directions of the GaN (0001) surface. Figure 2 shows such area, where the Ti-enriched regions appear brighter in the Ti

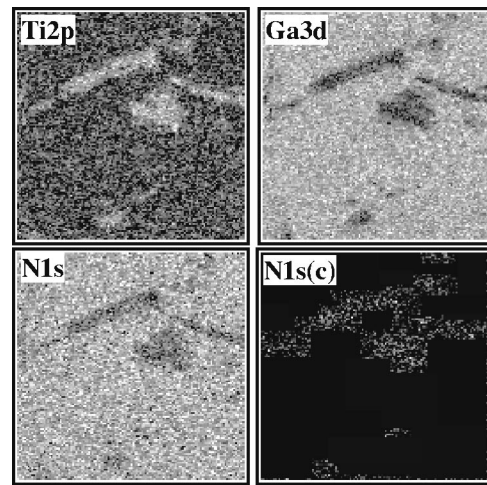


FIG. 2. Ti2p, Ga3d, and N1s images ($64 \times 64\ \mu\text{m}^2$) of areas with lateral chemical heterogeneity. The N1s(c) image is obtained after correction of the N 1s image for the attenuation effect of the Ti film.

2p map and darker in the Ga 3d and N 1s maps (due to stronger damping of the Ga 3d and N 1s emission from GaN by the locally thicker Ti film). After correction for the attenuation effect only the contrast of the N 1s image inverts (see N1(c) in Fig. 2), indicating that the Ti-enriched regions contain slightly more N as well. This spatial heterogeneity of the interface can be attributed to the presence of “defect” regions in the GaN films,²⁵ which are more reactive and act as agglomeration centers for Ti. From the attenuation of the Ga 3d emission from GaN we evaluated that the Ti film in the Ti-enriched regions can become two times thicker ($\sim 10\ \text{Å}$). The lateral heterogeneity manifested by the images in Fig. 2 is by no means a general phenomenon. In fact the Ti/GaN interface was dominated by large uniform areas covered with a 5 Å Ti film. Similar enrichment of “defect” areas with metal was also observed for Au/GaN and Ni/GaN interfaces after annealing and onset of interfacial reaction.^{17,18}

The immediate onset of a chemical reaction after RT deposition of Ti is manifested by the spectra in Fig. 1, namely growth of a new component in the Ga 3d spectra, R-Ga; and by two-component Ti 2p line shape, resembling the Ti 2p spectra of Ti nitrides ($\text{TiN}_{x=0.5-1}$), in which the intensity of the higher BE component increases with increasing x .²⁶ In both regions the BE of R-Ga is lower than that measured for a thick Ga metallic film deposited on GaN (18.6 eV). In addition to the higher local Ti and N concentration spectral features that distinguish the Ti-enriched regions are the higher intensity and the more pronounced BE shift of the R-Ga, plotted as a function of temperature in Figs. 3(a) and 3(b). The different BE of R-Ga indicates non-equivalent coordination of Ga with Ti, Ga and N atoms, e.g., spatial variations in the stoichiometry and in the structure of the metallic layer, which can be described as a ternary TiN_xGa_y phase. The N in the formed Ti nitride phases induced only a broadening of the N 1s spectra (not shown here), a bit more pronounced in the spectra from the Ti-enriched areas.

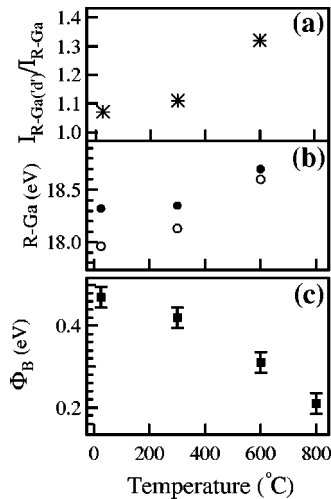


FIG. 3. Plots of the intensity ratio, $I_{R-Ga(3d)}/I_{R-Ga}$, between R-Ga from Ti-enriched and the remaining areas (a) the evolution of the BE of R-Ga from the Ti-enriched (open circles) and the remaining areas (filled circles) (b) and BB changes, Φ_B , (c) as a function of temperature.

Step annealing of the Ti/GaN interface up to 800 °C (temperatures up to 900 °C are used in semiconductor industry to form stable contacts in nitride devices) leads to further degradation of the GaN top layers and formation of a phase approaching the TiN stoichiometry. This was evidenced by the evolution of the Ti 2*p* spectrum, in which the higher BE Ti 2*p* component gained weight in both regions [Fig. 1(b)], and by the increased intensity of the N 1*s* signal (not shown). With increasing temperature the R-Ga approaches the BE of metallic Ga [see Fig. 3(b)]. The R-Ga disappears after annealing to 800 °C due to Ga evaporation and the Ga 3*d* spectra become identical to that of GaN. The contrast level of the Ga 3*d* maps observed at RT (Fig. 2) undergoes very small changes even after annealing to 800 °C, indicating that the abruptness of the interface and the differences in the local film thickness are not substantially affected by the temperature-induced transformations. We tentatively attribute this to a low mobility of the metallic TiN compound. This is a notable difference compared to the behavior of the Au/GaN (Ref. 17) and Ni/GaN (Ref. 18) interfaces, where upon annealing only Au(Ni)-Ga alloying occurs accompanied by penetration of Ni and Au atoms in the GaN lattice.

The Ti-induced band bending, Φ_B , in the different regions is plotted in Fig. 3(c) as a function of temperature. Since the Ti nitride related features cannot be unambiguously resolved in the N 1*s* spectra, only the Ga 3*d* shifts of GaN were used for evaluation of Φ_B . Each point is obtained from Ga 3*d* spectra measured in four Ti-enriched regions (at least 2 spectra per region) and several spectra taken randomly in the remaining area. The Φ_B values are corrected for surface photo voltage effect (SPV), caused by the high flux density, ($\sim 10^9$ photon/secin 0.01 μm^{-2} spot), used in SPEM experiments.^{13,27} For the Ti/GaN interface, where the evolving metallic layer has a distinct FL, the SPV-induced band flattening was easily corrected by alignment to the position of the equilibrium FL. The FL of the Ti-enriched regions

always coincided with the equilibrium one, while a SPV up to 0.15 eV was measured in the rest areas. Since in SPEM experiment the leakage current caused by SPV is due to bias between the illuminated microspot and the adjacent nonilluminated areas, the lateral variations of the SPV reflect a non-uniform conductivity of the interface. The absence of SPV in the Ti-enriched regions can be explained by the lower resistivity of the thicker metallic film. Figure 3(c) shows that Φ_B decreases with annealing temperature, i.e., with increasing N content due to the conversion of the TiN_xGa_y phase into TiN. The Φ_B decrease contradicts the electronegativity model,²⁸ which predicts an increase of Φ_B with the accumulation of electronegative N atoms. The occurrence of a chemical reaction accounts for this discrepancy. Changes in the stoichiometry of the metallic TiN_xGa_y phase undoubtedly affect the bonding configuration of the film to GaN surface and in turn the interfacial dipole. Creation of N vacancies in the top GaN layers will also contribute to the BB movements.

The most striking result is that after each treatment the same Φ_B values were measured in the different regions despite the differences in the film thickness and chemical composition, as manifested by the same Ga 3*d* energy position of GaN in Fig. 1(a). Considering also the difference in the local reactivity it is unlikely that the atomic arrangement and defect density of GaN layer in contact with the film is uniform. The negligible influence of the chemical lateral heterogeneity on the local BB appears to be a characteristic feature of M/GaN interfaces, since Au/GaN and Ni/GaN interfaces show the same peculiar behavior.^{17,18} This finding is rather unexpected considering the reported strong dependence of the SB height on the work function and structure of the M/GaN interface.^{7,11,15} None of the existing models can easily explain the experimental evidence of lateral variations of the microscopic morphology on both the metal and semiconductor side of the interface occurring on a length scale larger than the width of the depletion zone, and the homogeneous bend bending.

We explain the observed insensitivity of the SB by mutual interactions between the different regions. We assume that spatially separated regions have different Φ_B , but when they are in contact the requirement that the metallic layer should be equipotential leads to homogenization of Φ_B . Let us suppose that there is a Φ_B difference between two adjacent regions, which creates a potential bias. In the presence of a large density of free carriers lateral charge redistribution will occur, smoothing the potential fluctuations. Thus the local BB would be determined not only by the specific morphology of the interfacial layer but also by the lateral charge exchange between the different interface regions. In fact the homogenization of the potential fluctuations at the semiconductor *surface* in contact with the metal should have more general validity; it is a natural consequence of both the presence of a metallic layer and the metallization of the top semiconductor layers (due to metal induced gap states and/or subsurface penetration of the metal). However the charge transfer across the surface can be inhibited in systems with strong FL pinning such as nonintimate interfaces on contaminated semiconductor surfaces. We would like to stress that the constant Φ_B at the semiconductor surface, measured with

our extremely surface-sensitive method and the suggested charge redistribution mechanism does not exclude lateral variations of the potential deeper into the space-charge region.

In summary, we observed by photoelectron microscopy that the local SB height is insensitive to the lateral chemical heterogeneities at metal/GaN interfaces and have readdressed the mechanisms governing the built-up potential at M/S interfaces. We interpret our findings in terms of charge redis-

tribution leading to homogenization of the SB fluctuations at the semiconductor *surface*. Systematic investigations of other M/S systems are necessary to find out if the insensitivity of band bending at semiconductor surfaces to the microscopic interfacial morphology is limited to Me/GaN interfaces or is a more general phenomenon.

We are grateful to E. Bauer for the illuminating discussions and to D. Lonza for the technical support. The work was supported by Sincrotrone Trieste, grant EW15.

-
- ¹See for instance, *Metallization and Metal-Semiconductor Interfaces, Vol. 195 of NATO Advanced Study Institute, Series B*, edited by P. Batra (Plenum, New York, 1989); W. Mönch, *Semiconductor Surfaces and Interfaces*, Springer Series in Surface Sciences, edited by G. Ertl (Springer-Verlag, Berlin-Heidelberg, 1995).
- ²R.T. Tung, Phys. Rev. B **45**, 13 509 (1992).
- ³J.H. Werner and H.H. Güttler, J. Appl. Phys. **69**, 1522 (1991).
- ⁴M. van Schilfgaarde, E.R. Weber, and N. Newman, Phys. Rev. Lett. **73**, 581 (1994).
- ⁵A. Ruini, R. Resta, and S. Baroni, Phys. Rev. B **56**, 14 921 (1997).
- ⁶C. Berthod, J. Bardi, N. Binggeli, and A. Baldareschi, J. Vac. Sci. Technol. B **14**, 3000 (1996).
- ⁷S. Picozzi *et al.*, Phys. Rev. B **61**, 16 736 (2000).
- ⁸L.D. Bell and W.J. Kaiser, Phys. Rev. Lett. **61**, 2368 (1988).
- ⁹M. Prietsch and R. Ludeke, Phys. Rev. Lett. **66**, 2511 (1991).
- ¹⁰A.A. Talin *et al.*, Phys. Rev. B **49**, 16 474 (1994).
- ¹¹L.D. Bell *et al.*, Appl. Phys. Lett. **76**, 1725 (2000).
- ¹²K. Horn, Appl. Surf. Sci. **166**, 1 (2000).
- ¹³M. Kiskinova, M. Marsi, E. Di Fabrizio, and M. Gentili, Surf. Rev. Lett. **6**, 265 (1999).
- ¹⁴M. Kiskinova, Surf. Interface Anal. **30**, 464 (2000).
- ¹⁵S.J. Pearton, J.C. Zopler, R.J. Shul, and F. Ren, J. Appl. Phys. **86**, 1 (1999).
- ¹⁶K. Shiojima *et al.*, J. Vac. Sci. Technol. B **17**, 2030 (1999).
- ¹⁷A. Barinov, L. Casalis, L. Gregoratti, and M. Kiskinova, Phys. Rev. B **63**, 085308 (2001).
- ¹⁸A. Barinov *et al.*, Appl. Phys. Lett. **79**, 2752 (2001).
- ¹⁹M. Marsi *et al.*, J. Electron Spectrosc. Relat. Phenom. **87**, 149 (1997).
- ²⁰C.I. Wu *et al.*, J. Appl. Phys. **83**, 4249 (1998).
- ²¹J. Ma *et al.*, Appl. Phys. Lett. **69**, 3351 (1996).
- ²²Min-Ho Kim *et al.*, Phys. Rev. B **61**, 10 966 (2000).
- ²³W.R.L. Lambrecht *et al.*, Phys. Rev. B **50**, 14 155 (1994).
- ²⁴V. Fiorentini, M. Methfessel, and M. Scheffler, Phys. Rev. B **47**, 13 353 (1993).
- ²⁵S.C. Jain, M. Willinder, J. Narayan, and R. van Overstraeten, J. Appl. Phys. **67**, 965 (2000).
- ²⁶L. Porte, L. Roux, and J. Hanus, Phys. Rev. B **28**, 3214 (1983).
- ²⁷M. Marsi *et al.*, J. Electron. Spectrosc. Relat. Phenom. **94**, 149 (1998).
- ²⁸W. Mönch, J. Vac. Sci. Technol. B **17**, 1867 (1999).